Journal of Food Measurement and Characterization (2022) 16:1688–1701
https://doi.org/10.1007/s11694-021-01261-6

ORIGINAL PAPER

Identification of starch with assorted shapes derived from the fleshy root tuber of *Phoenix sylvestris*: extraction, morphological and techno-functional characterization

Achyuta Kumar Biswal[1] · Shriya Mishra[2] · M. B. Bhavya[3] · Akshaya Kumar Samal[3] · Ramchander Merugu[4] · Mithilesh Kumara Singh[5] · Pramila Kumari Misra[1]

Received: 27 May 2021 / Accepted: 13 December 2021 / Published online: 28 January 2022

Abstract

Currently, the starch of edible tubers from underutilized plants has been receiving considerable attention among starch manufacturers for versatile applications because of the abundance, cost-effectiveness, and biodegradability. The present study reports the isolation of a white-coloured crystalline starch of high purity (96.18 g 100 g^{-1}) from the fleshy root tuber of wild palm, *Phoenix sylvestris*, through water treatment and its characterization by different analytical techniques, such as Fourier transform infrared spectroscopy, X-ray diffraction spectroscopy (XRD), differential scanning calorimetry (DSC), Scanning electron microscopy (SEM) and thermal gravimetric analysis (TGA). The physicochemical analyses revealed the amylose content of the starch to be 62.39 g 100 g^{-1}. Through XRD probing the crystallinity and nature of starch were determined to be 22.12 ± 0.21% and B-type, respectively. The SEM analysis detected the assorted shapes of starch with a granular size in the range of 1–10 µm. The formation of unique flowery-shaped starch granules due to the complexation with protein through noncovalent interaction was also evident from the SEM image. From the DSC and TGA studies, the gelatinization parameters such as the onset (T_0), peak (T_p), complete gelatinization (T_c) temperatures, and enthalpy for the starch isolate were determined as 68.19 ± 0.02 °C, 82.27 ± 1.12 °C, 95.03 ± 0.15 °C, and 11.29 ± 0.01 J g^{-1}, respectively. The increase in enthalpy value of the retrogradation process on longer storage times demonstrated the higher reorganization of starch components. The characteristic temperatures of the retrogradation process were lower than the corresponding gelatinization process temperature. The scavenging of DPPH and ABTS radicals by the candidate starch confirmed its antioxidant properties. The overall studies indicated that the isolated novel starch could ascertain the applications in the production of biodegradable films for food packaging, preparation of syrups with high glucose content, as well as its incorporation into cooked and canned products.

Keywords Antioxidant activity · B-type starch · FTIR characterization · Gelatinization enthalpy · Retrogradation process · Starch-protein complex

✉ Pramila Kumari Misra
pramilamisra@rediffmail.com

[1] Centre of Studies in Surface Science and Technology, School of Chemistry, Sambalpur University, Jyoti Vihar, Sambalpur 768019, Odisha, India

[2] P.G. Department of Food Science & Technology and Nutrition, Sambalpur University, Jyoti Vihar, Sambalpur 768019, Odisha, India

[3] Centre for Nano and Materials Sciences, Jain University, Jakkasandra, Kanakpura Taluk, Ramanagara, 562112 Bangalore, India

[4] Department of Biochemistry, Mahatma Gandhi University, Nalgonda 508254, India

[5] Department of Chemistry, Patna University, Patna, Bihar 800005, India

Introduction

The consistent rise in population and the pollution thereof entails the development of materials that are sustainable, biodegradable, and economically viable [1–4]. In particular, the development of materials from the underutilized plant resources is highly beneficial because these resources are plentiful and inexpensive [5, 6]. Starch is a complex carbohydrate molecule with prospective utilization as a nutritional component in the human diet, a thickening agent in bakery products, an additive in paper manufacturing, and film for food packaging, and many more [7]. Literature survey reveals that the physicochemical and functional properties of starch depend on the origin of the sources, and hence its applications are designed accordingly [8]. The granule size and its distribution, mineral content, and amylose/amylopectin ratio largely determine the functional properties of starch biomolecules [8]. The small-sized starch granules, for instance, perform as lipid substitutes in the food systems and pharmaceutical industries due to better mouth feel [9] whereas on being complexed with proteins, the flavor, texture, shelf life, and digestibility of the finished food products get modified significantly [10]. The literature discloses that the formation of ternary starch-lipid-protein complexes alters the rheological behavior, pasting and gelatinization, and digestion rate of starch during food processing [11]. Thus, exploring novel starches and understanding their potential behaviors is of primary importance in developing real food matrixes [12]. Predominantly, starch is extracted from the roots, tubers, cereals, and legumes of different plants [1, 2]. Food components like wheat, corn, rice, and potatoes are rich sources of starch, and hence, these are frequently used for starch production [13]. Recent literature reports the isolation and physicochemical characterization of starch from indigenous roots and tubers of many plants such as *Coccinia abyssinica, Colocasia esculanta, Ensete veanirico-sum, Dioscorea abyssinica,* and *Plectranthus edulis* [14]. However, the judicious use of conventional sources and exploration of new botanical sources of starch is highly demanding and challenging to overcome the food security and overexploitation of the existing sources.

Palms are a group of perennial flowering plants of the Arecaceae family which grow as climbers, shrubs, tree-like, and stemless plants in tropical and subtropical climates [15]. These plants promise enormous utility in human nutrition, owing to the profuse nutritional content in their fruits, commonly known as a date [15, 16]. The nutritional contents of its fruits include sugar, minerals, phenolic and antioxidant component, and vitamins [17]. The pre-clinical studies have already revealed the potential medicinal properties of date fruit such as anti-mutagenic, hepato-protective, anti-inflammatory, anti-diabetic, anti-bacterial, anti-viral, anti-fungal, anti-tumor, nephro-protective, cardiovascular disease protective and anti-cancer properties [16]. Therefore, large varieties of palms are cultivated everywhere throughout the globe, and food products from the fruits are manufactured by the date industries [18]. Among all species, *Phoenix sylvestris*, commonly known as date palm, is a wild variety of palms that grows naturally as shrubs in southeast and western regions of Asia. This plant is used for the preparation of domestic articles such as ropes, baskets, and mats [17]. Its male plant never bears fruits, and the female plants do not bear quality fruit either. The tribal and local people use its raw fleshy roots tubers only as a low variety of food due to its rich content of starch, minerals, protein, when the plant is about 4 months old. Moreover, the plant growth and its survival remain unaffected after taking out the tubers also [16]. Thus, this plant remains mostly unutilized in general and particularly as non-productive from food perspectives contrasting the other palms plants under this family. Therefore, the isolation of value-added products from this wild variety of palms would be highly advantageous and cost-effective. The starch production from its tuber, unlike through the synthetic processes, would add least to the pollution profile, simultaneously fulfilling the requirements of the densely populated society. In addition, being a native starch, it could explore huge applications on modification of its functional groups [19].

With our continued interest for the product development using waste materials and underutilized resources [20–23], the present work reports the isolation of the starch from the fleshy root tubers of *P. sylvestris* by water treatment method and exploration of its physicochemical, structural, functional and thermal properties, and antioxidant activity. The results were compared with three common root starches of rhizome, cassava, arrowroot to recognize the potential of the isolated starch [24, 25].

Material and methods

Material

The fleshy root tubers samples were collected from a local farmer (Manpur Village, Bargarh, Odisha (India) during October 2018 and March 2019. Roots tubers were packed in polypropylene bags for further processing.

Starch extraction

The fleshy root tubers were washed, cut into small pieces, and ground with distilled water (1:10 ratio) in a blender (Vitamix 5200, India) for 4 min. The fibrous materials of the

homogenates were filtered out through three layers of mesh (140 µm, 50 µm, and 30 µm). The filtrates were allowed to settle at 4 °C for 24 h, and the supernatant was decanted. The starch cake residues were washed three times and dried at 40 °C in a hot air oven (Remi-RDHO 80, India) to get the dried palm tuberous root starch (abbreviated as PRS hereafter) [15]. The PRS was ground to powder and sealed in plastic bags for further studies. The yield of PRS was calculated as the ratio of the mass of the final product to the initial mass of palm root multiplied by 100. The extraction was repeated thrice to get the mean yield (in percentage) with the standard deviation.

Water activity, chemical composition, amylose content, and colour

The water activity of the PRS was analyzed with the help of a Electronic Thermo Hygrometer (IT202, India) at room temperature (25 °C) by the method described elsewhere [22]. The protein content was determined through the evaluation of nitrogen amount by the micro-Kjeldahl method and multiplying the resultant value with a factor of 6.25 [22]. The lipids were extracted out using hexane/petroleum ether in a Soxhlet apparatus. The ash content was determined through carbonization by a muffle furnace at 550 °C. The total dietary fibre was obtained by enzyme gravimetric method, and carbohydrate content was estimated by the difference [25]. The amylose content was determined using a method reported by Bento et al. [16]. The color parameters of the PRS were analyzed using a colorimeter (BC-10, Ramsey, USA) following the method from literature [26].

FTIR analyses

The FTIR spectrum of PRS was recorded by using an AVATAR 360 spectrophotometer (Thermo Electron, USA) using a KBr disc in the range 400–4000 cm^{-1} with a resolution of 4 cm^{-1} at 25 °C [27].

Morphology analyses

The morphology of PRS granules was analyzed using a scanning electron microscope (JEOL, JSM-6610, USA). The pre-hydrated powdered samples were fixed with double-sided tape onto aluminum supports and metalized with a 350 Å thick layer of gold for scanning. The scanned photographs were taken in triplicate using magnifications of 1000 to 10,000×. The particle size was determined using Image J (Version 4.5.0, LOCI, University of Wisconsin, USA) software with three replicates [28].

X-ray diffraction probing of PRS

The crystallinity of PRS was investigated with the help of an X-ray diffractometer (Shimadzu, XRD-6000) operating with Cu Kα radiation, 40 kV, 30 mA and a scanning speed between 10 °C and 40 °C (2θ). The analyte was dried for 24 h at ambient temperature and stored in a desiccator (containing silica as the dehydrating material). The degree of crystallinity was determined quantitatively following the equation-1, where A_c is the area of the crystallinity region of the X-ray diffractogram; A_a is the amorphous area of the X-ray diffractogram [25].

$$\text{Degree of crystallinity of the sample, Dc}(\%) = \frac{Ac}{Ac + Aa} \quad (1)$$

Thermal properties and pasting behaviour of PRS

Gelatinization of PRS

The gelatinization of the PRS followed by retrogradation was investigated with a differential scanning calorimeter (DSC-60 thermal analyzer, Shimadzu, Japan) and analyzed by Origin software 2018 version. following the procedure reported by Biswal et al. [26]. Approximately 2 mg of PRS was put into an aluminum crucible and mixed with 7.5 µL distilled water. Subsequently, the aluminum pan was sealed and equilibrated for 1 h at 4 °C. The inert atmosphere was maintained by passing nitrogen at 20 °C with flow rate at 20 mL min^{-1}. Gelatinization characteristics of PRS including onset temperature (T_o), peak temperature (T_p), endset temperature (T_c), and enthalpy of gelatinization (ΔH) were measured.

Thermal stability analysis

The thermal stability of PRS in the range 50–900 °C was obtained by a thermogravimetric analyzer (TGA, Perkin Elmer STA 6000, USA). The inert atmosphere was maintained by passing hot nitrogen gas (heated at 20 °C) with a flow rate of 20 mL min^{-1}.

Analysis of pasting property

The PRS of 2 g (d.w.b.) was dispersed in 20 mL of distilled water to get good dispersion in the water [29]. This dispersion was maintained at 50 °C for 1 min and then heated at 95 °C. The aliquot was held at 95 °C for 3 min and subsequently, cooled down to 50 °C at a speed of 11.84 °C min^{-1}. The peak viscosity, breakdown (viscosity drop), final

viscosity, and pasting temperature of the resulting sample were analyzed using a Rapid Visco Analyzer (Perten, RVA 4500, Perkin Elmer, India).

Water binding capacity, solubility and swelling power

The water-binding capacity (WBC) of PRS was determined following the method reported by Biswal et al. [26]. Approximately 1 g of dry PRS was mixed with 15 mL of distilled water in a centrifuge tube and shaken for 1 h using an orbital shaker (Model No. 3005, India). Thereafter, the sample was centrifuged at 16,366 g for 10 min. The supernatant in the centrifuge tube was discarded; the wet starch was drained out and then weighed.

The percentage of WBC was calculated using Eq. (2).

$$\mathrm{WBC}(\%) = \frac{Wet\ starch(g)}{Dry\ starch(g)} \times 100. \tag{2}$$

The solubility and swelling power of PRS were determined by the methods reported in the literature [25, 26]. The PRS was dried to constant weight (moisture content g/100 g) (d.w.b). 2.0 g of starch sample was transferred to a centrifuge tube containing 20 mL distilled water and heated in a water bath for 30 min at various temperatures (55, 65, 75, 85, and 95 °C). The sample was stirred at every 5 min with a vortex mixer (Digital Vortex Mixer, 120 V US/JP plug, Thermo Fisher Scientific) to ensure completer mixing. After cooling the starch sample up to 25 °C, the mixture was centrifuged at 16,366g for 10 min to separate the insoluble starch. The PRS was dried at 105 °C till the weight became constant. The mass of the lower layer (sediment) was used for the calculation of swelling power (SP). The following formulae were used to estimate S and SP, where A is the dry weight of the supernatant, W is the dry weight of the sample, and P is the weight of the sediment.

$$\mathrm{Solubility(S)} = \frac{A}{W} \times 100\%. \tag{3}$$

$$\mathrm{Swelling\ power(SP)} = \frac{P}{W \times (1 - S)}. \tag{4}$$

Antioxidant activity of the starch

The total phenolic content of PRS was measured using the Folin-Ciocalteu as per the method described in the literature [30, 31]. The 0.4 mL of 10% Folin-Ciocalteu solution was added to 0.2 mL of the aqueous starch suspension. After 5 min, 0.8 mL of the 10% sodium carbonate was added. Then the mixture was allowed to stand for 1 h at room temperature in the dark condition, and the absorbance was measured at 750 nm using a UV–Visible spectrophotometer. The total phenolic content was expressed as GAE (gallic acid equivalent)/g^{-1} d.w.b. The antioxidant activity was examined through the scavenging assay of DPPH and ABTS radicals [21]. The antioxidant activity of these two radicals was correlated with the phenolic content of PRS.

Statistical analyses

The data on the proximate composition, amylose content, gelatinization temperature, crystal type, degree of crystallinity, and retrogradation degree of PRS were obtained three times for each sample. The statistical analysis (ANOVA) was performed by the Duncan test (SPSS for Windows, Version 16) to determine the significance of the difference. The averaged data obtained along with mean (±) standard deviation are presented in the concerned tables.

Results and discussion

Physicochemical characteristics of PRS

Yield

The yield of PRS collected from the two seasons was analyzed. The analysis reveals that the yield of PRS extracted from the samples collected during March 2019 (21.68 ± 0.08 g 100 g^{-1} (d.w.b.) was higher than that collected in October 2018 (8.09 ± 0.12 g 100 g^{-1} (d.w.b), indicating the seasonal fluctuation of yield. Literature also reveals that physicochemical composition of starch is affected by the environmental conditions during the starch maturation [32] Further, since starch is essential storage of sugar required for sprouting, its deposition is higher during the predormancy period (when the growth of the plant is arrested) than the resprouting periods [33]. The yield envisages that PRS is a good source of starch similar to that of rhizomes roots reported by Bento et al. [34] (22.0 ± 0.3 g/100 g^{-1} (d.w. b)), but is smaller than that obtained from the roots of cassava (30 g/100 g^{-1}) and arrowroot (24.23 g/100 g^{-1}) [35, 36]. However, since the plant is underutilized, naturally grown and profusely available, it could be a profitable raw material for concerned product formation. Further, since the tree is perennial, wild, and does not produce quality fruits, the production of starch from its root could be highly cost-effective. The starch collected during March was subjected to different physicochemical, functional properties analyses. The physicochemical properties of the PRS are demonstrated in Table 1.

Table 1 Proximate composition of PRS

Constituent[a]	Average	Standard deviation	Coefficient of variation (%)
Moisture	6.34	0.0005	0.005
Ash	0.76	0.0001	0.032
Lipid	ND	ND	ND
Protein	1.97	0.0012	0.010
Carbohydrate	85.29	0.0051	0.300
Dietary fibers	0.09	0.0001	0.312
Amylose	62.39	1.12	2.122

ND not determined

[a]g 100 g^{-1}

Colour

The analysis of colour reveals that it is a white powder product with a luminosity of 91.41 ± 0.13, slightly yellowish, with chromaticity coordinates of a* of − 0.73 ± 1.16, b* of 6.78 ± 1.32, a hue angle of 96.08° ± 0.67 (yellow with a slight greenish color), and chroma of 6.29 ± 0.44 (pale color of low intensity). The colour of the raw starch predominantly decides the quality of starchy food products. Thus, white colour with higher luminosity values reflects the lightness and purity of the PRS, which could, therefore, be best suited for various foods, pharmaceutical, and textile industries applications [29].

Water activity and moisture content

Water exists in two forms in food, i.e., bounded water (moisture content) and free water(water activity, a_w). These two are not synonymous with each other. Usually, the more the moisture content of food, the greater is the water activity though it is not always the same. Sometimes the water activity differs much between two foods having the same moisture content [37]. It is, therefore, essential to determine both these parameters of starch for food applications. The a_w of PRS and moisture content of PRS were found to be 0.37 ± 0.01 and 6.34 g 100 g^{-1} at 25 °C, respectively. On comparison, the a_w of PRS is found to be much smaller than the starch of rhizomes (0.49 ± 0.01), cassava (0.60 ± 0.13). The a_w promotes the growth of fungi, bacteria, and yeast in food which in turn affects the colour, aroma, flavor, texture, stability, and quality of food [25, 38]. Further, it is an energy term that decides the escaping tendency of a water molecule from the food to the environment [37]. Thus, the low value of a_w, confirmed its better microbiological stability in comparison to these two established starches. The moisture content of PRS is also found to be much lower in comparison to the starches isolated from many other sources like the tubers of *Vigna angularis, Pueraria thomsonii, Discoria pyrifolia* plants [29]. The higher moisture content leads to the early microbial spoilage of the food [39]. The recommended moisture ranges for safe storage are less than 13% [40]. Thus, PRS could be the suitable commercial precursor for new food product development with greater food safety, longer shelf-life, quality, stability, and technological performance [41, 42].

Carbohydrate, protein, ash, and fiber

The carbohydrate content of PRS is estimated to be 85.29 g 100 g^{-1} (w.w.b.) or 96.18 g 100 g^{-1} on a dry weight basis (d.w.b). The ash (0.76 g 100 g^{-1}) and protein (1.97 g 100 g^{-1}) contents are quite low. Thus, the PRS with low protein and high carbohydrate is of high purity and quality [31]. The low content of dietary fibers (0.09 g 100 g^{-1}) and absence of lipid is due to the adoption of the sedimentation technique during the extraction [43]. The ash content in PRS exceeds slightly the limit recommended for the industry (0.5%), [44, 45]. The ash content in tubers of rhizomes and arrowroot plants are found to be 0.28% and 0.40% respectively [24, 34]. The ash content in PRS is, however less than some of the other reported tuber-starches (e.g. 0.88% ash content for tuber starch of *Dioscurea pyrifolia*) [45]. The ash content is the inorganic residue left after complete combustion of starch in air during the physicochemical analysis. The higher limit of ash content signifies that PRS contains higher acid- insoluble components like carbonates, silicates and oxalates [46]. The ash content signifies the presence of minerals in starch which retard the growth of the microorganism. Therefore, it can be used for a variety of starch-based food formulation. Further, it can be also used as herbal drug which allows 6–9% of ash content [47].

Amylose

The amylose content of starch depends on the different environmental factors and genotypes of the plants from which it is isolated [48]. It influences the chemical and functional characteristics of the starch. Therefore, analysis of amylose content is essential for the formulation of food products. The average amylose content of the PRS is found to be 62.39 g 100 g^{-1} (Table 1), which is higher than many of the starch reported in the literature thus, confirming the suitability of the extracted starch for the production of several dietary food products [25, 29, 39]. The presence of high amylose content facilitates the formation of gel, which is indispensable for the formulation of pasta, bread, sweets, and coating materials [49]. The processes like starch granule swelling, gelatinization, and retrogradation abilities depend on the amount of amylose content of the starch [50]. The high content of amylose is advantageous for the film, bio-membrane, coating purposes, which require low permeability to water and

good oxygen barrier properties. The presence of amylose in food products also reduces insulin and glycemic response, the risk of obesity, cardiovascular disease, and the development of type II diabetes [42]. Thus, in view of high amylase content, the extracted starch could be a promising precursor for versatile applications.

Structural and morphological characteristics of PRS

FTIR analyses

Starch is a natural polymer with applications in the nutritional, biomedical, and industrial sectors. The native starch has, however, limited applications. But the functional groups present in the native starch polymer is modified through chemical reactions to suit a large number of the desired applications [19, 51]. Generally, starch possesses a large number of the characteristics of functional groups, such as carboxyl, acetyl, hydroxypropyl, amine, amide groups. But the occurrence of these groups varies from species to species depending on the origin and environment of the sources [52]. It is, therefore, essential to identify the functional groups present in a novel starch molecule to explore its possible applications. FTIR spectroscopic analysis is an established technique to identify these functional groups. Further, for robust characterization, it is necessary to have a comprehensive understanding of the 'fingerprint' region, in which the molecular vibrations are very specific to the molecular species. The mid-infrared region is the fingerprint region: this region is so-called because most organic molecules and inorganic substances have characteristic absorption in this region. Figure 1 represents the FTIR spectrum of PRS. The spectrum clearly envisages the polysaccharide's nature of the starch [53]. The broad spectral band within the region 3000 and 3500 cm^{-1} confirms the presence of the O–H group associated with water molecules [54]. The peak at 2935 cm^{-1} represents C–H stretching, the intensity of which depends on the variations in the ratio of amylose and amylopectin in starch. The water absorbed in the amorphous part of the starch granules band appears at 1653 cm^{-1}. The fingerprint region of the spectrum corresponds to the stretching of the functional group C–O in the range 1500–600 cm^{-1}. The peak at 1402 cm^{-1} in the fingerprint region corresponds to symmetric stretching of the carboxyl group –COOH [54, 55]. The peak at 1361 cm^{-1} signifies the C–H angular deformation. The sharp peaks at 1167 to 1021 cm^{-1} are assigned to the coupling modes of C–O, C–C stretching, and C–O–H bending modes [56]. The peaks at 990 cm^{-1} (due to C–O bond stretching) and 867 cm^{-1}(due to C–O–C group vibration) confirm the presence of the anhydroglucose ring in the starch [54–56]. The peaks at 921 and 767 cm^{-1} indicate the skeletal mode vibration of α-1, 4, glycosidic linkage, and C–C stretching, respectively [25]. Bands at 567 and 511 cm^{-1} are attributed to the skeletal modes of the pyranose ring in the glucose unit of starch [56]. The spectral region from 500 to 1200 cm^{-1} originates mainly from carbohydrate vibrations. The pattern of the IR spectrum authenticates the purity of the starch isolates. For industrial point of views, the PRS can be used as viscosifiers, emulsifiers, defoaming agents, for encapsulation and as sizzing agents.

XRD study

The XRD pattern of PRS is illustrated in Fig. 2. In the diffraction spectrum, three intense diffraction peaks at 2θ value of 15.09°, 17.36°, and 23.32° are distinctly observed. Generally, semi-crystalline starch granules exhibit three types of XRD pattern. Literature studies report that most of the cereal starches show A-type XRD pattern with reflections at 2θ of 15° and 23° and doublet peaks at around 2θ of 17° and 18°

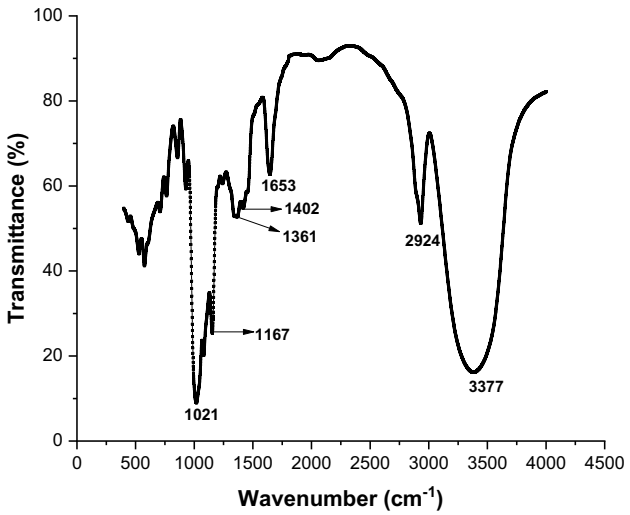

Fig. 1 FTIR spectrum of PRS

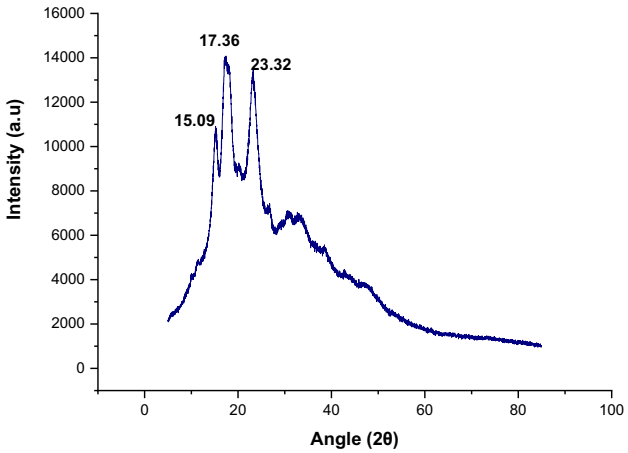

Fig. 2 XRD pattern of PRS

[39] whereas. the B-type XRD pattern with reflections at around 17° and minor reflections at around 5.6°, 15°, 20°, 22°, and 24° as the 2θ is seen in case of most of the root and tuber starches. On the other hand, the C-type starch shows superposition of both A and B-type patterns with strong reflections at about 17° and 23° as the 2θ value; and a few minor reflections at around 5.6° and 15° as the 2θ values, depending on the proportion of A- and B-type allomorphs [39]. Considering these facts, it is clearly evident that PRS belongs to B-type of starch. Using Scherer equation, the degree of crystallinity was quantitatively estimated as the ratio of the diffraction peak area and total diffraction area [3]. This value comes out to be 22.12 ± 0.21% for PRS. This value is much lower than cassava starch (31.90 ± 0.12%), arrowroot starch (42.00 ± 0.01%) but is higher than isolated rhizome starch (17.05 ± 2.41%) [25, 41, 42, 57].

The starch consists of the linear amylose and branched amylopactin polymers. These two polymers form the complex structure in such a way that the semicrystalline and amorphous regions occur alternatively to give rise to the A-category of starch with granules that are partially crystalline [57]. The double helices of amylopectin constitute the crystalline region, whereas the amorphous region is formed by the amylose chains. The amylose chains are intermingled among the branched chains of amylopectin. Thus, amylose content does not contribute to the crystallinity of starch [58]. The crystal size, extent of crystalline regions, orientation of the double helices within the crystalline domains, and the interaction of double helices in the starch granules decide the crystallinity of starch [59]. Since PRS has a semi-crystalline structure, it can contribute better to the texture, stability, quality, and digestibility of the food products.

Scanning electron micrographs (SEM) analysis

SEM image demonstrates the morphology of material; specifically, it indicates the size and shape of the material [25]. These two characteristic features depend on the geographical origin [60] and comprehensively control the thermal and functional properties of the starch polymer. Therefore, the determination of these parameters is necessary before setting for applications.

The SEM image of PRS (Fig. 3) clearly indicates the variable shape, and size of the granule. Under the low magnification of 2000×, the majority of the granules appear either oval or spherical-shaped. At times, a novel flower-shaped starch (Fig. 3d) was prominently detected under the high magnification, i.e., 8000×. Since the functional properties of starch are dependent on the shape and crystallite size, the unique PRS extracted by us could ascertain more applications towards food development [61]. The average granule size of PRS lies within 1 to 10 µm. The literature also reports

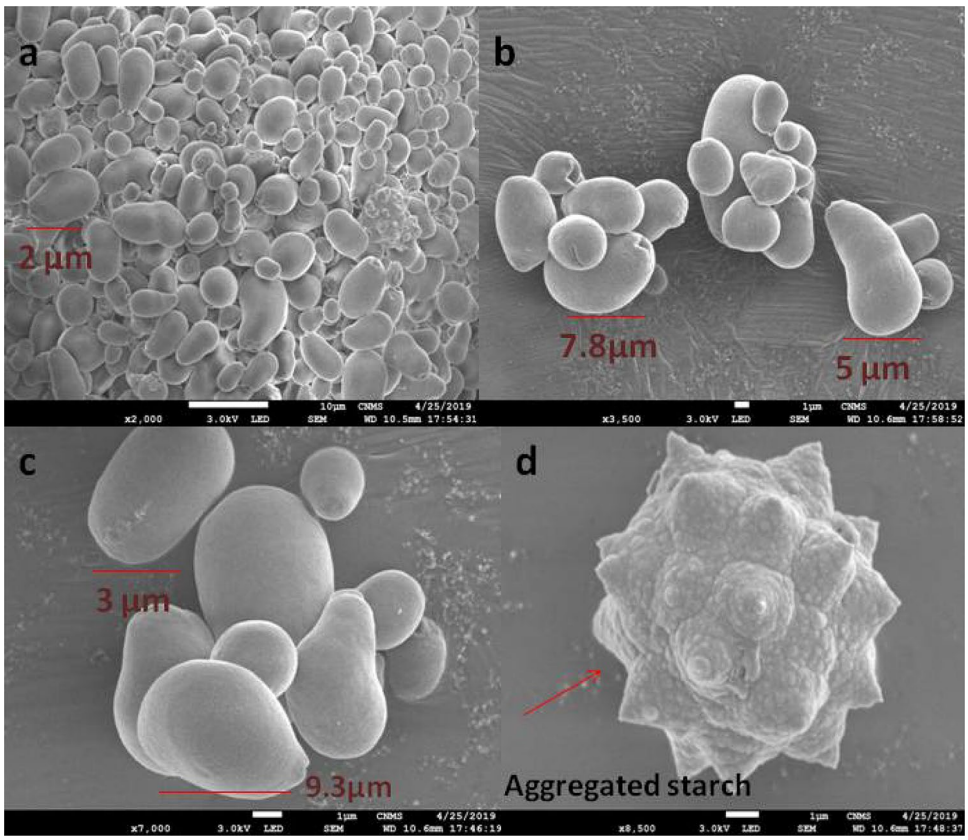

Fig. 3 SEM images of PRS under different magnifications; **a** 2000×; **b** 3500×; **c** 7000×; **d** 8500×

some of the starches with size within this range [62]. The A-type starch granules are typically disk-like or lenticular in shape with diameters ranging from 10 to 35 µm. On the contrary, B-type granules are roughly spherical or polygonal in shape, ranging from 1 to 10 µm in diameter. Thus, the starch isolated in the present work is mostly B-type granules, which is significantly correlated with physicochemical properties such as amylose content, water binding capacity and swelling power of PRS [63]. The flowery shape structure of PRS may be due to the formation of aggregates of starch with the small amount of protein present content (1.97%). FTIR envisages the presence of CH regions in starch which may interact with the fatty patches of protein [64] through hydrophobic interactions. Hydrogen bonding between the functional groups of starch and protein may also strengthen the complex formation [65, 66]. Such assorted shapes of starch due to the presence of protein and lipids have been reported in literature [67]. The functional and nutritional properties of such as digestibility, texture, shelf life, and flavor of finished food products are affected remarkably due to the formation of these aggregates. The complex formation reduces the swelling power and solubility of starch, retards the gelatinization and retrogradation, and slows down the rate of enzymatic digestion of the food products [68]. These complexes can also encapsulate the bioactive to protect the latter from autoxidation and degradation: as a result, the potential activity of the bioactive is increased [67, 68]. The PRS can be a good precursor for food applications.

Thermal behaviour of PRS

Gelatinization

The gelatinization of starch is a process in which the disruption of the double helix (amylose region) and melting of the crystalline regions (amylopectin) of the starch granules occurs in the presence of water and heat [43]. The starch granules are semi-crystalline in nature, and on heating with water, they swell via an endothermic process increasing the randomness of the starch simultaneously [43]. On dissolution of the granules, the texture of the starch softens and its digestibility increases. Hence, gelatinization is an essential process during the development of starchy food products. The gelatinization process is, however, reliant on the amylose and amylopectin content in the starch, and hence, it is a characteristic property of the starch [69]. This phase transformation in PRS is evident from the thermal heating curve shown in Fig. 4a. The characteristic parameters of gelatinization, i.e., on set (T_o), peak (T_p), endset (T_c), temperatures and the range temperature, R ($R = T_c - T_o$) for PRS were found to be 68.19 ± 0.02, 82.27 ± 1.12, 95.03 ± 0.15, and 26.84 ± 1.09 °C, respectively with a gelatinization enthalpy (ΔH) of 11.29 ± 0.01 J g^{-1} (Table 2). The ΔH value (also regarded as heat flow), quantitatively represents the loss of molecular order within the starch granule due to the gelatinization phenomenon. Several factors, such as the amylose content, size, shape, aqueous solubility of starch, efficiency of starch to bind the water molecule, and the internal arrangement of the starch decide the magnitude of the ΔH value. The lower organization within the starch granule yields a smaller ΔH value. On the other hand, the high degree of crystallinity in starch results in high transition temperature. In such a case, the structure of starch becomes highly stable, and therefore, the starch granule experiences a greater resistance during gelatinization. Thus, the difference in transition temperatures accounts for the extent of the degree of crystallinity of starch. Similar trends of the gelatinization parameters in the case of the cassava root starch, arrowroot starch, and rhizome starch have been reported in the literature [24, 62, 70, 71]. The higher temperature range

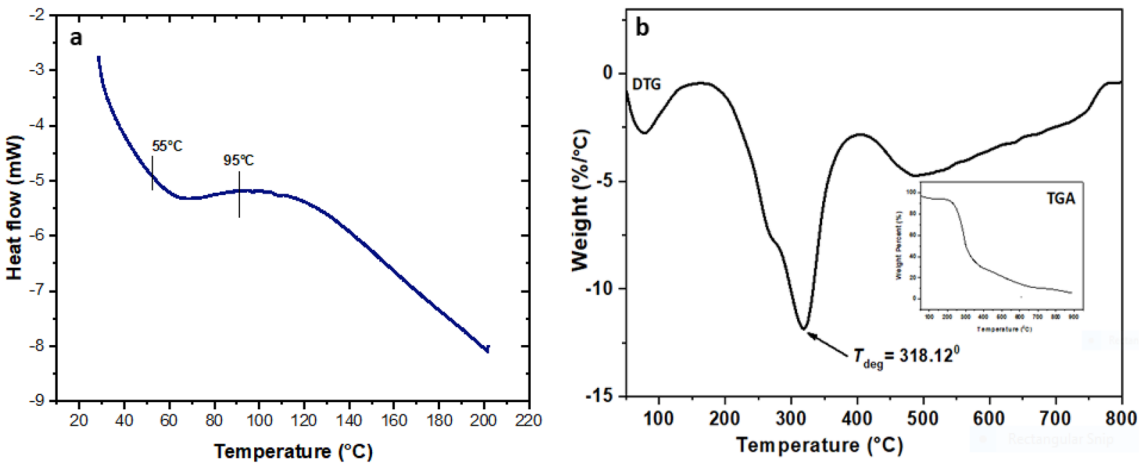

Fig. 4 Thermal curves of PRS: **a** DSC curve showing gelatinization temperature; **b** Thermogravimetric differential thermal analysis (TGDTA curve showing degradation temperature (Inset:TGA curve)

Table 2 Gelatinization temperature, crystal type, degree of crystallinity and retrogradation parameters of PRS

Palm root starch	T_0 (°C)	T_p (°C)	T_c (°C)	ΔH (J g^{-1})	R (%)	Crystal type	Degree of crystallinity (%)	RD (%)
Gelatinization	68.19 ± 0.02	82.27 ± 1.12	95.03 ± 0.15	11.29 ± 0.01	26.84 ± 1.09	A	22.12 ± 0.21	ND
Retrogradation (7 d)	53.82 ± 1.01	73.32 ± 0.09	79.81 ± 0.09	1.60 ± 1.34	25.99 ± 0.05	ND	ND	14.17 ± 0.26
Retrogradation (14 d)	52.13 ± 2.01	71.89 ± 3.11	82.25 ± 0.10	1.91 ± 0.11	30.12 ± 3.01	ND	ND	16.91 ± 1.32
Retrogradation (21 d)	59.33 ± 0.07	75.11 ± 1.29	84.65 ± 0.67	2.89 ± 0.21	23.32 ± 1.13	ND	ND	25.59 ± 0.05

The results are given as the mean of three determinations ± standard error of the mean

On set (T_o), peak (T_p), endset (T_c), Δ*H* gelatinization enthalpy, *R* gelatinization range ($T_c - T_0$), *RD* retrogradation degree (RD) = (retrogradation ΔH/gelatinization Δ*H*) × 100

ND not determined

(R) and gelatinization enthalpy (Δ*H*) of PRS in comparison to the other starch species suggest the presence of crystalline regions of different strengths in granules [25, 59, 62, 72].

Starch retrogradation

During the starch retrogradation, the disordered amylose and amylopectin chains in gelatinized starch assume a more ordered and compact structure. The bound water gets released, the phenomenon being alternatively termed as syneresis [62]. The ratio and structure of amylose and amylopectin, the concentration of the starch, geographical origin of starch, water content, storage conditions, and temperature of the medium decide the rate of starch retrogradation [73]. Thus, the starch retrogradation is advantageous for the formation of starchy food products in terms of textural and nutritional properties and helps in the storage of starchy foods [74].

The retrogradation process of PRS was investigated at different storage conditions (after 7, 14, and 21 days) of the gelatinized PRS. The results are presented in Table 2. On examination, it is seen that the transition temperatures, i.e., on set (T_o), peak (T_p), endset (T_c), enthalpy change (Δ*H*), and gelatinization range percentage are lower than those in gelatinization temperature of PRS. The higher enthalpy value (Δ*H*) of retrogradation starch during the longer storage times indicates the higher reorganization of starch components. This is desirable for the longer shelf-life of the food products. This happens because of the less orderly rearrangement of amylopectin during storage at low temperatures [25, 74].

Thermogravimatry analysis of PRS

The thermogravimetric analysis (TGA) assesses the thermal degradation behavior and thermal stability of starch. The thermal degradation of PRS was studied in the range 50 to 800 °C. Figure 4b represents the thermal properties of the isolated PRS by derivative thermogravimetry (Thermogravimetric differential thermal analysis, TG–DTA) envisaging three different zones of weight loss. The first zone of weight loss of mass between 50 and 130 °C (Zone I) corresponds to the dehydration of water bound to the sample. The second and major weight loss between 267 and 379 °C (Zone II) represents the degradation of amylose and amylopectin chain breakage, while the third weight loss region lies in the range of 385–480 °C (Zone III) due to the oxidation of organic matter [43]. The single narrow and intense peak of the DTG curve indicates that rapid degradation reaction occurs at low temperature range i.e. from 300 to 335 °C. The thermal decomposition temperature of PRS was found to be 318.12 ± 0.12 °C. The degradation activity is also reported around the same temperature for cassava (335.52 ± 0.35 °C), arrowroot (330.00 ± 0.11 °C) and rhizome starch (316.94 °C ± 0.24 °C), respectively [24, 25, 75]. The PRS does not decompose within 190 °C, and therefore, has superior thermal stability, which is good for the development of starchy food products [25].

Pasting properties

After gelatinization, the starch absorbs water and forms a paste. Several factors, such as the amylose content, hydration capacity of the granules, amylose leaching, and molecular structure of the amylopectin, amylose–lipid complexation, and stiffness of the granules determine the pasting property of starch [25]. Usually, the branched amylopectin chains evidently tend to have a high pasting temperature and low viscosity peaks, because the chains are too short to maintain the stiffness of the granules [76].

The pasting temperature of the PRS determined through rheological analysis was found to be 71.05 °C ± 0.11 as against the values of 77.8, 67.4 and 73.92 °C for arrowroot, cassava and rhizhomes starches, respectively [77]. The pasting temperature is thus, close to the initial gelatinization temperature of 68.19 °C ± 0.02 obtained from the endotherm in the DSC analysis of PRS (Fig. 4a). A good correlation was also obtained between gelatinization and pasting

temperatures. The different characteristic parameters like peak viscosity, final viscosity and minimum viscosity were found to be 1824 ± 43 cP, the 2887 ± 21 cP, and 1967 ± 59 cP, respectively which are similar to that reported for cassava starch [78]. The high value of the final viscosity indicates a greater expansion capacity of the starch granules during the gelatinization process and may be related to high amylose content. Final viscosity also contributes stability and rigidity to the granular structure of starch [78]. The high pasting temperature with the low viscosity peak of PRS suggests that PRS is more stable during the heating and cooling process.

Functional properties of PRS

Water binding capacity

The water-binding capacity (WBC) of starch refers to the ability of starch to absorb water and hold it even after treatment with external forces. The large numbers of hydroxyl groups present in starch help in holding the water molecules through the hydrogen bonding. In addition, the starch chains and the diverse granular structure also monitor the water binding capacity of PRS [25]. The chains of amylose and amylopectin interact weakly with water at room temperature. But when the temperature rises, the thermal energy weakens the hydrogen bonds, which in turn boosts up the interaction of the starch chains with water. This results in the assimilation of starch and water [69]. The WBC of PRS was calculated to be 3.11 ± 0.01, which is higher than the WBC of roots of cassava (0.90 ± 0.23) and lower from that isolated from the roots of rhizome (90 ± 0.02), respectively [54, 71, 79].

Solubility and swelling power

The aqueous solubility of starch is a critical parameter that decides its use towards various products. Since it is not an ionic compound, its aqueous solubility depends primarily on the interaction of water either through H-bonding with the large number of –OH group present on its molecular framework or its ability to non-covalently bind with the water molecules [25, 80]. The solubility parameter reflects the extent of amorphous and crystalline domains, i.e., on the amylose-amylopectin ratio, degree of branching and length of the branched amylopectin chain, distribution of these two sugar units with respect to mass and types [25]. Besides these factors, the knowledge on the amount of lipid and protein in the starch, the extent of self-interaction of its branched chains are also divulged from the water solubility parameter [29]. In particular, these values are the signature of the amylose content, the ability of the starch to hold water molecule, the extent of the hydrogen bonding, disruption of the starch structure, and the degree of crystallinity of the starch. The interactions between amylose-amylose and amylose-amylopectin chains also influence the solubility and swelling parameters [81]. Thus, determining these two parameters, information on the molecular structures, granule sizes, and botanical sources can be congregated [81].

Figure 5 shows the solubility and swelling power of PRS at 55–95 °C. On examination of the trend of these two values, an intensification of both these parameters with the temperature is noted through a radical increase at 75–95 °C. The water solubility and swelling power of the starch vary from 18.24 ± 0.11 to 36.76 ± 0.05, and 6.31 ± 1.19 to 29.72 ± 0.21, respectively. These solubility and swelling power are much higher in comparison to arrowroot starch (1.59 ± 0.60 to 17.22 ± 1.43% and 2.17 ± 0.21 g g^{-1} to 11.32 ± 0.53 g g^{-1}), cassava starch (1.62–71.15% and 2.22–15.63 g g^{-1}) and rhizome species (2.11 ± 0.01 to 13.08 ± 0.12 g g^{-1} and 5.11 ± 0.11 to 17.24 ± 0.12%) within the same temperature ranges [24, 54, 71, 79]. The results indicate that, when the temperature increases from 75 to 85 °C, the ability to absorb water and dissolution of the starch in the water conspicuously increases: the initial gelatinization temperature of starch also increases at 75 °C (Fig. 5). The swelling property of PRS also corroborates with the above temperature and is consistent with the DSC analysis. These results indicate that PRS is comprised of long amylopectin chains linked with the high amylose content (Table 1) and therefore, it has moderate swelling power. The high solubility in water at a lower temperature may eventually facilitate to be used as an additive in food products perfectly.

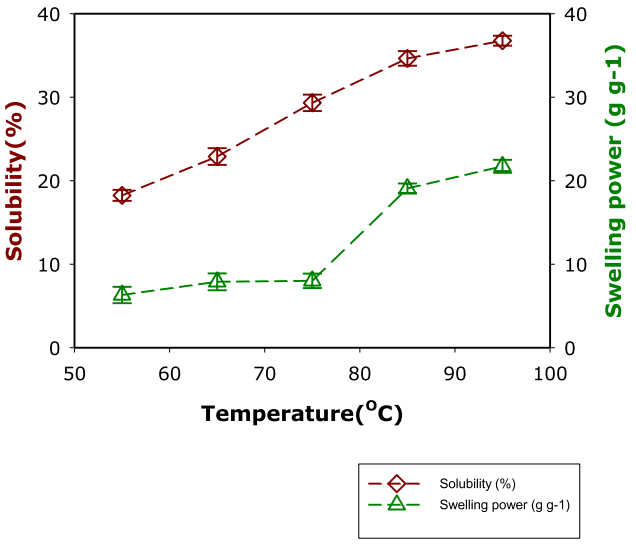

Fig. 5 Plots of solubility (%) and swelling power (g/g) of PRS as a function of temperature

Bioactive properties of PRS

One of the most significant bioactive properties of starch phenols is represented by their antioxidant activity, which is exploited to preserve the stability and quality of the food products. The oxidative degradation through complex radical mechanism is the primary cause of the spoilage of the food product [82]. Due to this degradation phenomenon, the nutritional values of the food like fatty acids, proteins, lipids, soluble vitamins get degraded, causing ultimately the indigestion of these food products [21]. The physical conditions like odour and colour of the food also deteriorate. In some cases toxic materials are generated [82]. Therefore, controlling the degradative oxidation is an essential stipulation for the preservation of the food products. This requires trimming down the bioavailability of the superfluous reactive radicals formed during different metabolic processes [83]. Starch contains a large number of phenolic –OH group that can oxidize these reactive radicals through the mechanism similar to the biological oxidation–reduction reaction occurring within the biological system [84]. Thus, the bioactive property of starch can be exploited to increase the stability of food products. In order to account for this activity of PRS, the antioxidant activity of PRS was determined through forage of two commonly used radicals, DPPH and ABTS as a function of its phenolic content, as demonstrated in Fig. 6. As is indicated from the plot, the total phenolic content, DPPH, and ABTS activity of PRS values increase with the increase of the dose of PRS in the medium. On increasing the PRS amount in the aqueous extract from 2 to 10 g mL^{-1}, the percentage of phenolic content increased from 20.44 ± 0.11 to 30.91 ± 2.01 whereas, the percentage of antioxidant activity of DPPH and ABTS increased from 29.70 ± 1.21 and 24.51 ± 0.13 to, 51.85 ± 2.31 and 42.64 ± 2.12, respectively. The total phenolic content and the antioxidant capacity assays are also statistically significant ($p < 0.05$). Thus, it is seen that with the increasing concentration of starch, the phenolic content and free radical scavenging activity of PRS increased uniformly. Literature studies do not correlate the phenolic content and antioxidant activity of the conventional starches such as cassava, potato, maize, arrowroot, etc. However, few studies report the polyphenolic content of starch on their functional behaviors such as rheology, gelatinization, retrogradation, morphology, and paste [85–88]. So, the PRS has potential phenolic compound which may help in development of food production or act like as efficient antioxidant. The increased antioxidant activity of starch (a polysaccharide) might be due to the breakdown and depolymerization by radiolysis to low molecular weight subunits that lead to the exposure of their -OH groups and decreasing the intramolecular hydrogen bonding. This also correlates well with the FTIR analysis (Fig. 1) [86]. Similar type of observation has been reported by Mukhtar et al. [87]. Thus, the bioactive property analysis of PRS suggests that it can be applied as antioxidant in food and pharmaceutical industries, and for food packaging processes.

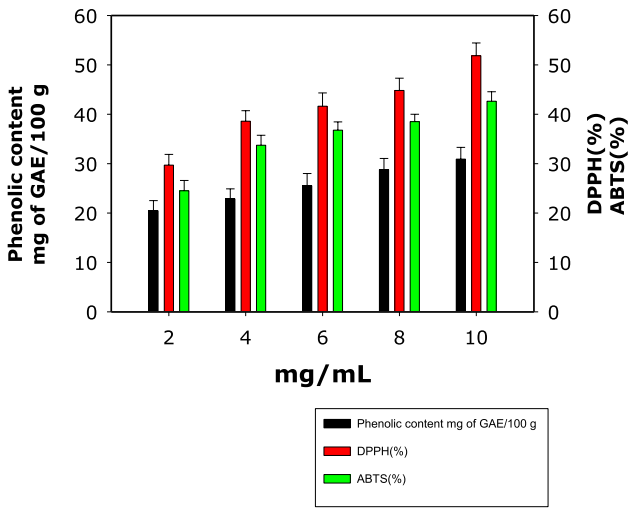

Fig. 6 Plots of phenolic content, DPPH and ABTS scavanging activities as a function of PRS amount

Comparison with starches reported in literature

Table 3 represents a comparative analysis of the physicochemical properties along with the gelatinization temperature, crystal type, degree of crystallinity, and granule size of the different common starches reported in literature with our present study [89–93]. The analysis clearly envisages that most of the characteristic parameters of the PRS correlate with the other common starches very well. The amylose content is, however, significantly higher, which can, therefore, facilitate the formation of the stable amylose–lipid complex. This complex influences the thermal properties of the starch. Moreover, the granule size is also appreciably similar to the other starches [60]. The granule size is amenable for enzymatic hydrolysis, enzymatic binding, and reaction [88]. The gelatinization temperature of PRS is found to be higher in comparison to the other. This could be more beneficial as, under this condition, the hydrogen bonds formed between the water molecules with amylose and amylopectin can break thereby, exposing its hydroxyl groups. This would promote its water solubility [25]. Thus, PRS may have greater potential in the development of different food products in comparison to the other.

Conclusion

During these days, product development using waste materials and underutilized plants is receiving considerable attention due to the abundance and cost-effectiveness of

Table 3 Comparative analysis of physiochemical, thermal and crystal nature of PRS with the reported starches in literature

Sample	Moisture (%)	Ash (%)	Protein (%)	Amylose (%)	Gelatinization temperature (°C)	Crystal type	Degree of crystallinity	Granule size (μm)	References
Cassava	16.50	0.31	0.52	26.20	70.90	A	30	5–35	[64]
Potato	13.67	0.26	1.82	27.00	72.65	B	28	1–110	[64–66]
Sweet potato	9.33	0.28	1.13	0–65	79.10	A	30	2–42	[25]
Maize	13.65	0.54	2.20	0–84	67.00	A	41.8	35.0	[67, 68]
Wheat	10.00	0.60	6.44	25.95	83.10	A	36	6–25	[64]
Sorghum	9.20	0.14	0.28	14.0–23.7	68–72		35–38	5.5–30	[69]
Tapioca	8.10	0.70	4.98			A	42	5–25	[39]
Palm root tuber (PRS)	6.34	0.76	1.97	62.39	82.27	A	22.19	10 to 35	The present study

the raw materials. The present study describes the isolation, characterization of a novel starch from the roots of underutilized wild date palm (*Phoenix sylvestris*) and investigation of its physical, morphological, thermal, and functional characteristics for prospective applications in foodomics, biomedical and industrial fields. The XRD pattern confirmed the crystal of palm root starch to be 'B' type. The shape of the starch was found to be oval and spherical. A distinct flowery structure was also sporadically detected under high magnification due to the aggregation of starch with protein through non-covalent interactions. The granular size of the starch was found to lie between 1 and 10 μm. The TG–DTA studies indicated that the starch isolates can withstand up to 190 °C. The gelatinization study demonstrated the initial, peak, complete gelatinization temperatures of starch. The enthalpy value increases during the retrogradation study, confirming the higher reorganization of starch components on storing longer time. The characteristic temperatures of retrogradation were found to be lower than that of the corresponding temperatures of the gelatinization process. The antioxidant character of the starch was established from the DPPH and ABTS scavenging assays. Thus, the isolated starch has the appropriate chemical-structural, thermal and technological properties for suitable exploitation as a precursor for food and non-food materials such as crispy food, coating materials, hydrogels, films, bio-membranes, and adhesives. The ability to form aggregates with proteins ascertain its possible applications in drug delivery and control-release of bioactive molecules. Although the correlation between the structures of starch with its functional properties has progressed significantly, still its utility in drug delivery, food packaging, and slurry stabilization remains obscure to date. Exploration of new starches and their chemical/physical modifications for desired applications still holds challenges that need to be resolved through consistent investigation, innovation, and execution.

Acknowledgements Financial supports of the UGC (No.F.540/14/DRS/2013 (SAP-I)) and DST (SR/FST/CSII-021/2012(G)) to the School of Chemistry are gratefully acknowledged. Support of TRIFED, Govt. of India (TFD/HO/R&D/2016-17/20/ Vol-3/4279), New Delhi to PKM and senior research fellowship to AKB is also gratefully acknowledged.

References

1. F.D. Guerra, M.F. Attia, D.C. Whitehead, F. Alexis, Molecules **23**, 1760 (2018)
2. A. Samant, B. Nayak, P.K. Misra, J. Environ. Chem. Eng. **5**, 5429–5438 (2017)
3. B. Nayak, P.K. Misra, Mater. Chem. Phys. **230**, 187–196 (2019)
4. B. Nayak, P.K. Misra, Mater. Chem. Phys. **239**, 121967 (2020)
5. S. Parida, D.K. Sahu, P.K. Misra, Energ Source Part A. **38**, 1110–1116 (2016)
6. D. Das, S. Panigrahi, P.K. Misra, A. Nayak, Energ Fuel. **22**, 1865–1872 (2008)
7. R.N. Tharanathan, Crit. Rev. Food Sci. Nutr. **45**, 371–384 (2005)
8. Y. Wang, G. Zhang, Food Res. Int. **140**, 110009 (2021)
9. S. Siddiqui, N. Dalal, A. Srivastva, A.K. Pathera, J. Food Meas. **15**, 2805–2820 (2021)
10. S. Wang, C. Chao, J. Cai, B. Niu, L. Copeland, S. Wang, CRFSFS **19**, 1056–1079 (2020)
11. R.A. Gonzalez-Soto, B. de la Vega, F.J. García-Suarez, E. Agama-Acevedo, L.A. Bello-Pérez, LWT Food Sci. Technol. **44**, 2064–2069 (2011)
12. Á. Bravo-Núñez, R. Garzón, C.M. Rosell, M. Gómez, Foods **8**, 155 (2019)
13. N. S. M. Yazid, N. Abdullah, N. Muhammad, H. M. Matias-Peralta, J. Sci. Technol. **10**, (2018)
14. B. Dereje, Int. J. Biol. Macromol. **187**, 911–921 (2021)
15. M. Oves, M. Aslam, M.A. Rauf, S. Qayyum, H.A. Qari, M.S. Khan, I.M. Ismail, Mater. Sci. Eng. C. **89**, 429–443 (2018)
16. P. Jain, S. Jain, S. Sharma, S. Paliwal, Agri. Nat. Resour. **52**, 107–114 (2018)
17. M. Jonoobi, M. Shafie, Y. Shirmohammadli, A. Ashori, H.Z. Hosseinabadi, T. Mekonnen, J. Renew. Mater. **7**, 1055–1075 (2019)
18. M. Chandrasekaran, A.H. Bahkali, Saudi J. Biol. Sci. **20**, 105–120 (2013)
19. D. Singla, A. Singh, S.B. Dhull, P. Kumar, T. Malik, P. Kumar, Int. J. Biol. Macromol. **163**, 1283–1290 (2020)

20. L. Panda, S. K. Jena, S. S. Rath, P. K. Misra, Environ. Sci. Pollut. Res. 1–15 (2020)
21. A. K. Biswal, P. K. Misra, Mater. Chem. Phys. 123014 (2020)
22. A.K. Biswal, P.K. Panda, J.M. Yang, P.K. Misra, IET Nanobiotechnol. **14**, 654–661 (2020)
23. J. Meher, D. Das, A.K. Samal, P.K. Misra, Mater. Today: Proceed. **9**, 542–550 (2019)
24. G.F. Nogueira, F.M. Fakhouri, R.A. de Oliveira, Carbohydr. Polym. **186**, 64–72 (2018)
25. J.A.C. Bento, K.C. Ferreira, A.L.M. de Oliveira, L.M. Lião, M. Caliari, M.S.S. Júnior, Int. J. Biol. Macromol. **135**, 422–428 (2019)
26. A.K. Biswal, C. Lenka, P.K. Panda, J.M. Yang, P.K. Misra, LWT Food Sci. Technol. **137**, 110459 (2020)
27. A.K. Biswal, A.K. Samal, M. Tripathy, P.K. Misra, Mater. Today: Proceed. **9**, 605–614 (2019)
28. C.A. Schneider, W.S. Rasband, K.W. Eliceiri, Nat. Methods **9**, 671–675 (2012)
29. C.K. Reddy, F. Luan, B. Xu, Int. J. Biol. Macromol. **105**, 354–362 (2017)
30. M.M.S. Ismaiel, Y.M. El-Ayouty, M. Piercey-Normore, Braz. J. Microb. **47**, 298–304 (2016)
31. A. Kamboj, R. Gupta, A. Rana, R. Kaur, Europ. J. Biomed. Pharma. Sci. **2**, 201–215 (2015)
32. O. O. Kunle, Chemical Properties of Starch, BoD–Books on Demand, **35**, 1–14 (2019)
33. Y. Von Fircks, L. Sennerby-Forsse, Tree Physiol. **18**, 243–249 (1998)
34. J. A. C. Bento, M. C. Fidelis, M. A. de Souza Neto, L. M. Lião, M. Caliari, M. S. S. Júnior, Int. J. Biol. Macromol. **145**, 332–340 (2020)
35. M.S.A. Fakir, M. Jannat, M.G. Mostafa, H. Seal, J. Bangladesh Agri. Univ. **10**, 217–222 (2012)
36. O. F. Vilpoux, V. H. Brito, M. P. Cereda, Starches for Food Application, (Academic Press, 2019), pp.103-165
37. R.K. Tadapaneni, R. Yang, B. Carter, J. Tang, Food Res. Int. **102**, 203–212 (2017)
38. T.H. Mu, M. Zhang, *Sweet potato starch* (In Sweet Potato, Academic Press, 2019), pp. 27–68
39. Y. Zhong, Y. Wu, A. Blennow, C. Li, D. Guo, X. Liu, LWT-Food Sci. Technol. **134**, 110176 (2020)
40. E. Kamau, C. Mutungi, J. Kinyuru, S. Imathiu, C. Tanga, H. Affognon, K.K.M. Fiaboe, Food Res. Int. **106**, 420–427 (2018)
41. K. S. Trinh, T. B. Dang, Int. J. Food Sci. 1–7 (2019)
42. J. Man, J. Cai, C. Cai, H. Huai, C. Wei, Carbohydr. Polym. **89**, 571–577 (2012)
43. P.S. Hornung, R.C.T. Barbi, G.L. Teixeira, S. Avila, F.L.D.A. da Silva, M. Lazzarotto, R.H. Ribani, J. Therm. Anal. Calorim. **134**, 2075–2088 (2018)
44. J. A. Radley, Starch and its derivatives (3rd ed.), (New York: John Wiley and Sons, 1953) **1**, pp. 369–401
45. M.E. Sharlina, W.A. Yaacob, A.M. Lazim, S. Fazry, S.J. Lim, S. Abdullah, M. Kumaran, Food Chem. **220**, 225–232 (2017)
46. K. Rakholiya, S. Chanda, Asian Pac. J. Trop. Biomed. **2**, 680–684 (2012)
47. S.S. Ajazuddin, Pharmacogn. Res. **2**, 318 (2010)
48. L. Fu, L. Liu, W. Chen, Q. Wang, X. Lv, J. Wang, X. Zhang, LWT-Food Sci. Technol. 109694 (2020)
49. I.G. Cordelino, C. Tyl, L. Inamdar, Z. Vickers, A. Marti, B.P. Ismail, LWT-Food Sci. Technol. **99**, 1–7 (2019)
50. R.S. Policegoudra, S.M. Aradhya, Food Hydrocoll. **22**, 513–519 (2008)
51. D. Das, U. Dash, A. Nayak, P.K. Misra, Energy Fuels **24**, 1260–1268 (2010)
52. S.W. Kariuki, J.W. Muthengia, M.K. Erastus, G.M. Leonard, J.M. Marangu, Heliyon **6**, 04574 (2020)
53. I. Cumpstey, Int. Scholarly Res. Notices, 1–27 (2013)
54. K. Jamir, K. Seshagirirao, Food Hydrocoll. **72**, 247–253 (2017)
55. R. Kizil, J. Irudayaraj, K. Seetharaman, J. Agri. Food Chem. **50**, 3912–3918 (2002)
56. F.J. Warren, M.J. Gidley, B.M. Flanagan, Carbohydr. Polym. **139**, 35–42 (2016)
57. K. Dome, E. Podgorbunskikh, A. Bychkov, O. Lomovsky, Polymers **12**, 641 (2020)
58. W. Shujun, L. Hongyan, G. Wenyuan, C. Haixia, Y. Jiugao, X. Peigen, Food Chem. **99**, 30–37 (2006)
59. R. Hoover, W.S. Ratnayake, Food Chem. **78**, 489–498 (2002)
60. Y.I. Cornejo-Ramírez, O. Martínez-Cruz, C.L. Del Toro-Sánchez, F.J. Wong-Corral, J. Borboa-Flores, F.J. Cinco-Moroyoqui, CyTA-J. Food **16**, 1003–1017 (2018)
61. D.S. de Castro, I. dos Santos Moreira, L.M. de Melo Silva, J.P. Lima, W.P. da Silva, J.P. Gomes, R.M.F. de Figueirêdo, Food Res. Int. **124**, 181–187 (2019)
62. D. de Souza Fernandes, T.P.R. dos Santos, A.M. Fernandes, M. Leonel, Int. J. Biol. Macromol. **132**, 710–721 (2019)
63. E.J. Vernon-Carter, J. Alvarez-Ramirez, L.A. Bello-Perez, C. Hernandez-Jaimes, I. Reyes, Starch-Stärke **72**, 1900087 (2020)
64. S. Maharana, P.K. Misra, J. Phy. Chem. B **122**, 5161–5172 (2018)
65. P.K. Misra, J. Meher, S. Maharana, J. Mol. Liq. **224**, 900–908 (2016)
66. P.K. Misra, U. Dash, S. Maharana, Collods. Surf. Part A Physico. Engg. Aspects **483**, 36–44 (2015)
67. J. Singh, L. Kaur, H. Singh, Adv. Food. Nutri. Res. 137–179 (2013)
68. M. Zheng, C. Chao, J. Yu, L. Copeland, S. Wang, S. Wang, J. Agri. Food Chem. **66**, 1872–1880 (2018)
69. D. Rengadu, A.S. Gerrano, J.J. Mellem, Int. J. Biol. Macromol. **147**, 268–275 (2020)
70. X. Li, W. Chen, Q. Chang, Y. Zhang, B. Zheng, H. Zeng, Int. J. Biol. Macromol. **144**, 67–75 (2020)
71. A.L. Charles, K. Cato, T.C. Huang, Y.H. Chang, J.Y. Ciou, J.S. Chang, H.H. Lin, Food Hydrocoll. **53**, 187–191 (2016)
72. K. Alvani, X. Qi, R.F. Tester, C.E. Snape, Food Chem. **125**, 958–965 (2011)
73. O. Patino-Rodriguez, E. Agama-Acevedo, G. Ramos-Lopez, L.A. Bello-Pérez, Food Hydrocoll. **101**, 105512 (2020)
74. Y. Tian, Y. Li, X. Xu, Z. Jin, Carbohydr. Polym. **84**, 1165–1168 (2011)
75. B. Jankovic, Carbohydr. Polym. **95**, 621–629 (2013)
76. F. Zhu, Food Hydrocoll. **63**, 332–348 (2017)
77. S. Srichuwong, T.C. Sunarti, T. Mishima, N. Isono, M. Hisamatsu, Carbohydr. Polym. **62**, 25–34 (2005)
78. D. Chandanasree, K. Gul, C.S. Riar, Food Hydrocoll. **52**, 175–182 (2016)
79. S.A. Oyeyinka, A.A. Adeloye, O.O. Olaomo, E. Kayitesi, Food Biosci. **33**, 100485 (2020)
80. P.K. Misra, H.P. Mishra, U. Dash, A.B. Mandal, J. Colloid Interface Sci. **333**, 590–598 (2009)
81. T. G. Hughes, Doctoral dissertation, Memorial University of Newfoundland (2013)
82. F. Shahidi, P. Ambigaipalan, J. Funct. Foods **18**, 820–897 (2015)
83. R.Z. Chen, L. Tan, C.G. Jin, J. Lu, L. Tian, Q.Q. Chang, K. Wang, Ind. Crops Prod. **77**, 434–443 (2015)
84. D. L. Nelson, A. L. Lehninger, M. M. Cox, (2008)
85. R.C.T. Barbi, G.L. Teixeira, P.S. Hornung, S. Ávila, R. Hoffmann-Ribani, Food Hydrocoll. **77**, 646–658 (2018)
86. P.S. Hornung, K. Masisi, L.N. Malunga, T. Beta, R.H. Ribani, Polym. Bull. **75**, 4735–4752 (2018)
87. R. Mukhtar, A. Shah, N. Noor, A. Gani, I.A. Wani, B.A. Ashwar, F.A. Masoodi, Int. J. Biol. Macromol. **104**, 1313–1320 (2017)

88. B.R. Ramadoss, M.P. Gangola, S. Agasimani, S. Jaiswal, T. Venkatesan, G.R. Sundaram, R.N. Chibbar, J. Food Sci. Technol. **56**, 391–400 (2019)
89. S. Ren, Starch-Stärke **69**, 1600367 (2017)
90. D. Stawski, Food Chem. **110**, 777–781 (2008)
91. N.W. Cheetham, L. Tao, Carbohydr. Polym. **36**, 277–284 (1998)
92. B. P. N. Phiarais, E. K. Arendt, In Gluten-free cereal products and beverages. (Academic Press, 2008), pp. 347–372
93. Y. Sang, S. Bean, P.A. Seib, J. Pedersen, Y.C. Shi, J. Agric. Food Chem. **56**(15), 6680–6685 (2008)